HHS Public Access

Author manuscript

Urology. Author manuscript; available in PMC 2024 May 13.

Published in final edited form as:

Urology. 2017 August ; 106: 133–138. doi:10.1016/j.urology.2017.04.020.

Near-Infrared Intraoperative Molecular Imaging Can Identify Metastatic Lymph Nodes in Prostate Cancer

Leilei Xia[1,2], **Ryan Zeh**[2,3], **Jack Mizelle**[2,4], **Andrew Newton**[2,4], **Jarrod Predina**[2,4], **Shuming Nie**[5], **Sunil Singhal**[2,4], **Thomas J. Guzzo**[1,2]

[1]Division of Urology, Department of Surgery, University of Pennsylvania Perelman School of Medicine, Philadelphia, PA

[2]Center for Precision Surgery, Abramson Cancer Center, University of Pennsylvania Perelman School of Medicine, Philadelphia, PA

[3]Department of Neurosurgery, University of Pennsylvania Perelman School of Medicine, Philadelphia, PA

[4]Division of Thoracic Surgery and Thoracic Surgery Research Laboratory, Department of Surgery, University of Pennsylvania Perelman School of Medicine, Philadelphia, PA

[5]Department of Biomedical Engineering, Emory University, Atlanta, GA

Abstract

Objective: To propose a novel method to perform indocyanine green (ICG) based near-infrared (NIR) fluorescence imaging during pelvic lymph node dissection (PLND) for prostate cancer patients with lymph node metastasis (LNM).

Materials and Methods: A prostate cancer cell line PC3 was used to establish xenograft model in NOD/SCID mouse. After tumor growth, mice were injected through the tail vein with ICG. Xenografts and surrounding tissues were imaged with NIR camera 24 hours after intravenous ICG and tumor-to-background ratios (TBRs) were calculated. We then performed a pilot human study to evaluate the role of NIR imaging in robotic PLND after systemic ICG in four patients with prostate cancer and preoperative lymphadenopathy.

Results: ICG localized to PC3 xenografts in the mice and all xenografts were highly fluorescent compared to surrounding tissues with a median TBR of 2.85 (interquartile range [IQR] = 2.64 – 3.90). In the human study, intraoperative *in vivo* NIR imaging identified three of the four preoperative lymphadenopathies as fluorescence positive and back table *ex vivo* NIR imaging identified all four lymphadenopathies as fluorescence positive. All the lymphadenopathies were

Correspondence information Thomas J. Guzzo, MD, MPH, Perelman Center for Advanced Medicine, West Pavilion, 3rd Floor, 3400 Civic Center, Boulevard Philadelphia, PA 19104, Fax: +1-215-662-3955, thomas.guzzo@uphs.upenn.edu.

Disclosure: No conflicts of interest

found to be LNMs by pathologic examination. Two of the four cases had additional LNMs, all of which were fluorescence positive with intraoperative *in vivo* NIR imaging.

Conclusions: Intravenously administered ICG accumulates in prostate cancers in both a murine model and human patients. NIR fluorescence based on intravenous ICG may serve as a useful tool to facilitate the identification of positive nodes during PLND in patients with higher risk of LNMs.

Keywords

prostatic neoplasms; lymph node excision; molecular imaging; indocyanine green

INTRODUCTION

Information regarding the presence of lymph node (LN) metastasis (LNM) is important for the staging and management of prostate cancer. Traditional imaging procedures such as CT and MRI have limited ability to predict LNM in a preoperative setting [1]. Currently, pelvic lymph node dissection (PLND) remains the most accurate staging procedure for the detection of LNM although the extent of PLND remains controversial [2]. Unfortunately, even extended PLND (ePLND) does not ensure complete accuracy regarding nodal status [3]. For patients with a higher probability of having LNM, such as patients with lymphadenopathy in radiological exams, it would thus be advantageous for the surgeon to have an additional tool that can be used to identify suspicious lymph nodes more consistently and reliably in the intraoperative setting. Recent studies have reported that salvage PLND after primary treatment might be a viable treatment option for patients with nodal recurrence, as it was found to prolong recurrence-free survival and delay systemic therapies [4, 5]. For this group of patients, efficient and precise intraoperative identification of targeted and suspicious LNs is clinically useful. Near-infrared (NIR) intraoperative molecular imaging has the potential to assist surgeons in the intraoperative identification of pathologic LNs [6].

For PLND in prostate cancer, one of the most commonly studied NIR tracers is indocyanine green (ICG). However, the majority of studies to date utilized intraoperative, intraprostatic injection of ICG [7–13]. This is perhaps a result of the origins of the tracer as an angiographic imaging agent. This technique poses several disadvantages, notably “dye spillage”, which leads to high background signals in the blood vessels and adjacent tissue [7, 14, 15]. Additionally, the drainage patterns of the prostate to the lymphatic system are very complex and have not shown distinct pathways, which might further impede the usage of intraprostatic injection of ICG [8].

Recently, our group has been studying a novel ICG injection technique known as second window ICG. Second window ICG refers to the delivery of higher doses of ICG intravenously 24 hours before surgery [16]. By delivering higher doses with this timing, this technique takes advantage of the enhanced permeability and retention (EPR) effect, which allows for the ICG to accumulate in solid tumors due to their more permeable vasculature and disorganized lymphatics [16–18]. Other preclinical and clinical studies utilizing this approach have shown utility in identifying various types of solid tumors, including glioma, lung cancer, thymoma, breast cancer, and metastases [16, 19–22]. In this study, we hypothesized that utilizing second window ICG will help the surgeon identify LNM in

prostate cancer. To test this, we established a murine prostate cancer model to determine if ICG can reach the tumors via the second window ICG. We then performed a pilot study using this method in four patients with known prostate cancer and lymphadenopathy.

MATERIALS AND METHODS

Cell lines

Human prostate cancer cell line PC3 was used. PC3 cells were grown in RPMI 1640 medium supplemented with 10% fetal bovine serum, 1% penicillin–streptomycin, and 1% glutamine. Cell cultures were maintained in 5% carbon dioxide (CO_2) at 37.0°C in a humidified incubator.

Murine xenograft model

The Animal Care and Use Committees of the Children's Hospital of Philadelphia and the University of Pennsylvania approved all procedures. Ten 6 to 8-week old NOD/SCID mice (Charles River Laboratories) were subcutaneously injected in the back or flank with 2×10^6 PC3 cells suspended in 100 μL of phosphate-buffered saline. Thirty to 40 days after inoculation (tumor size reached about 500 mm^3), mice underwent intravenous 5 mg/kg ICG injection through the tail vein before imaging. One day (24 hours) after the ICG injection, the mice were sacrificed by CO_2 asphyxiation and cervical dislocation and immediately underwent imaging to assess PC3 flank tumor fluorescence.

Human trial

The clinical trial was approved by the University of Pennsylvania Institutional Review Board, and all patients gave informed consent. Patients with biopsy-proven prostate cancer and suspicious enlarged pelvic lymph nodes (lymphadenopathy in radiological exams) were eligible for this study. As a pilot study, 4 patients were enrolled, including 2 patients scheduled for robot-assisted radical prostatectomy (RARP) with PLND, and 2 patients scheduled only for robotic PLND. Da Vinci Xi and Si were used for the surgeries. All patients received 5 mg/kg of intravenous ICG infusion through a peripheral vein one day before undergoing surgery. No adverse reactions related to the infusion were observed.

Near-infrared fluorescence imaging

In order to visually identify NIR fluorescence, two different machines were used. To image the murine tumor xenografts, the Visionsense Iridium (Visionsense, Philadelphia, Pennsylvania) camera was used. This system is FDA-approved for perfusion imaging in plastic and reconstructive surgery. It overlays NIR signal onto a high-quality visible light view and additionally provides the ability to view NIR signal only. ImageJ software (http://rsb.info.nih.gov/ij/, National Institutes of Health) was used to quantitate the tissue fluorescence. Using the NIR image generated by the Visionsense, a region of interest (ROI) was generated and placed around the fluorescent specimen to quantify the fluorescence. Fluorescence was measured in arbitrary units (A.U.) based on the number of photons that reached the camera detector. Tumor fluorescence was based on the entire tumor. Background readings were taken from surrounding subcutaneous tissue. Tumor-to-background ratios

(TBRs) were then generated. All readings were done in triplicate to generate an average value.

In order to visually identify the NIR fluorescence intra-operatively, the Firefly NIR system, which is built into the Da Vinci robotic platform, was used. During the operation (PLND), the surgeon toggled between the white light and Firefly NIR views. Due to limitations of depth of penetration in NIR imaging, proper tissue dissection was often performed before NIR imaging. In general, the goal was to see if NIR fluorescence was helpful in locating and identifying suspicious lymphadenopathy and other possible metastatic LNs. TBRs were not calculated based on *in vivo* tumor and lymph node visualization, as the Firefly software does not provide and "NIR-only" image, but an overlaid, green pseudocolor in real time. The Visionsense Iridium was again used to image the removed LN specimen *ex vivo* on the back table.

RESULTS

ICG localizes to PC3 xenograft tumors in mice

All mice survived to the day of imaging and were found to have tumors. Eight out of 10 tumors were fluorescent before exposing the tumor, and all tumors were highly fluorescent when compared to surrounding tissues after exposing the tumor (Figure 1). Median tumor fluorescence was 120 A.U. (IQR 102 to 140 A.U.) and median background fluorescence was 40 A.U. (IQR 34 to 55 A.U.). The median TBR calculated from these values was 2.85 (interquartile range [IQR] = 2.64 – 3.90). Fluorescence was also noted in the liver and intestines, which is consistent with hepatic metabolism and biliary excretion of ICG.

Human trial overview

In the human trial, all four patients tolerated the ICG infusion very well and successfully underwent the scheduled operations. Patient characteristics are shown in Supplementary Table S1. No conversion to open surgery or intraoperative complications occurred. Operative time was 65, 87, 33, and 140 minutes, respectively. Estimated blood loss was 50, 200, 50, and 200 ml, respectively. All patients were discharged on postoperative day one and no postoperative complications occurred.

NIR fluorescence of the lymphadenopathies in human trial

For patients with preoperative lymphadenopathy, final pathology confirmed metastatic LNs (adenocarcinoma) in all cases. *In vivo*, NIR imaging showed that all the enlarged LNs were fluorescent except for Case 1. Case 3 demonstrated the strongest fluorescence (Figure 2). A video clip of Case 3 is shown in Supplementary Video.

After *in vivo* imaging and PLND, all the LN specimens were imaged on the back table to assess NIR fluorescence before they were sent to pathology. The specimens containing the lymphadenopathy from Cases 1–3 were found to be fluorescent *ex vivo* (Figure 3). There was a camera malfunction during Case 4 and no *ex vivo* imaging was recorded.

NIR fluorescence of other LNs in human trial

Case 1, 2, and 4 underwent ePLND and additional LN specimens were retrieved. Final pathology showed that all the specimens had at least one LN. Case 1 had additional two positive LN specimens (right external iliac and right common iliac) which were found to be fluorescent *in vivo* (Figure 4). Case 4 had additional a positive LN specimen (left iliac) which was found to be fluorescent *in vivo*. *Ex vivo* imaging confirmed fluorescence in the specimens from Case 1. However, *ex vivo* imaging of the negative LN specimens also showed fluorescence. The results of NIR imaging and pathology are summarized in Supplementary Table S2.

COMMENT

In this translational study, we found that prostate cancer xenografts in mice will fluoresce after intravenous delivery of ICG 24 hours prior to NIR imaging. These results are consistent with other types of solid tumors [17, 20–22]. We then showed intraoperative NIR imaging after utilizing second window ICG can identify LNMs in patients. Based on the preliminary results of our study, we believe that intraoperative NIR imaging can serve as an additional tool in PLND for patients with prostate cancer, especially those with a higher risk of LNM and nodal recurrence.

We relied on a usage of second window ICG and subsequent NIR imaging. In general, systematically administered a high dosage of ICG have two peaks in terms of NIR fluorescence: the first is in vascular perfusion period (10 minutes) and the second is the EPR effect period (24 hours) [17]. Even though second window ICG involves higher dosage, it is still very safe [16, 19–22]. The median lethal dose (LD_{50}) of ICG is 80 mg/kg and the dosage we used is well below the LD_{50} [22]. Optimal timing (24 hours) and dosage (5 mg/kg) were based on our previous preclinical animal and clinical data [16, 17, 19–23]. This is the first study to demonstrate the feasibility and practicality of second window ICG based NIR fluorescence in PLND for prostate cancer.

Focusing on patients with radiological signs of LNM, we wanted to see if NIR fluorescence via the second window ICG could help the surgeon to identify and/or locate suspicious LNs during PLND. Our goal was to determine if the fluorescence was helpful in identifying cancer (LNMs), not non-cancerous LNs. Further investigation on the utility of this technique for patients without pathologically enlarged lymph nodes is necessary. We observed a few shortcomings in the translation of NIR signal from the dye to the imaging machine intraoperatively. In many situations, proper dissection was needed before high-quality NIR imaging could be achieved. NIR imaging platforms that have lower thresholds for signal detection could help to ameliorate this problem.

There have been multiple studies on fluorescence imaging in PLND. Most of the studies utilized intraprostatic injection of the dye and primarily focused on optical biopsy of sentinel LNs (SLNs) [7–13]. Several injection techniques have been proposed, including trans-rectal [8], trans-perineal [9, 11, 12], and direct visualization [7, 10, 13]. The ICG dosage, injection location, time interval from injection to image, imaging platform, and patient selection also varies among these studies. With so many variables, these types of studies are only further

complicated by the facts that 1) there is no well-agreed upon definition of SLN, and 2) the lymphatic draining pattern of the prostate is complicated and does not follow a distinct spreading pathway. This may be a contributing factor to the variations in diagnostic accuracy of NIR imaging for SLN detection [8, 11, 24, 25].

Two recent studies, in part, examined the sensitivity of detecting LNMs via intra-prostatic injection of ICG. Utilizing this ICG injection technique resulted in a low sensitivity to detect LNMs and a conclusion that ICG-based fluorescence for PLND does not represent an alternative to meticulously performed ePLND in higher risk patients [8, 11]. While our sample size was not large enough to draw definite conclusions, we believe that by using the second window ICG technique, which relies on the EPR effect, ICG-based NIR fluorescence has the potential to enhance PLND procedures, at the expense of potential false positives.

Second window ICG has the advantage in that it reduces variables in clinical studies. This includes standardized ICG delivery, less signal interference from “dye spillage”, fewer background signals, and more flexible time to image during surgery. We included only robotic PLND in the human trial considering both the dominant role of robotic surgery for prostate cancer and the fact that the robotic platform (Si and Xi) has the integrated Firefly system that can detect NIR fluorescence. The major advantage of the Firefly system is that the console surgeon can easily toggle between the white light and NIR fluorescence. However, its threshold for signal detection may be limited. Importantly, by utilizing our systematic ICG administration, our approach requires no extra setup during surgery and accordingly no added operative time.

Of note, we did not calculate the exact sensitivity of the results because of the limited number of patients and different camera systems used *in vivo* and *ex vivo*. However, of all the specimens imaged, we only encountered one false negative *in vivo* and no false negative *ex vivo*. Overall, it appeared that the *ex vivo* camera system (Visionsense) showed more positives than the *in vivo* Firefly system. Several potential explanations might account for the discrepancy between *in vivo* and *ex vivo*. First, it is possible that the *ex vivo* system has a lower signal detection threshold than Firefly. Second, fluorescence *in vivo* might be blocked by the surrounding tissue and fat. Third, the strength of the signal is partially dependent on the distance between the camera and the specimen. Although we standardized the distance *ex vivo* imaging and for TBR measurements, it was very hard to control the distance perfectly *in vivo*.

Given that current work is a pilot and proof-of-principle study with small sample size, further studies with a large sample size and appropriate study design are still needed to evaluate the diagnostic (sensitivity and specificity) and therapeutic (oncologic outcomes) performance of the second window ICG based fluorescence-guided PLND. Fluorescence-guided or fluorescence-enhanced PLND has been increasingly studied and might be a promising surgical approach for certain group of patients with prostate cancer. However, there is a pressing need to come up with some standardized approach in conducting future studies and reporting the results considering differences between these studies. Until then, the direct comparison of the diagnostic and therapeutic performances of various fluorescence-guided PLND techniques may not be accurate and meaningful. In

the meantime, development and clinical application of new tracers that specifically bind to prostate cancer will certainly be important to move forward [26–28].

CONCLUSIONS

Intravenously administered ICG accumulates in prostate cancers in both a murine model and human patients. NIR fluorescence based on second window ICG may serve as a useful tool to facilitate the identification of positive nodes during PLND in patients with higher risk of LNMs. However, studies with large sample size and further refinement are still needed before the true clinical value can be determined.

Supplementary Material

Refer to Web version on PubMed Central for supplementary material.

ACKNOWLEDGMENTS

Dr. Irfan Asangani from Department of Cancer Biology at the University of Pennsylvania kindly provided the cell line PC3.

Funding:

Supported by National Institutes of Health R01 CA193556.

References

1. Hovels AM, Heesakkers RA, Adang EM, et al. The diagnostic accuracy of CT and MRI in the staging of pelvic lymph nodes in patients with prostate cancer: a meta-analysis. Clin Radiol. 2008; 63:387–395. [PubMed: 18325358]
2. Briganti A, Blute ML, Eastham JH, et al. Pelvic lymph node dissection in prostate cancer. Eur Urol. 2009; 55:1251–1265. [PubMed: 19297079]
3. Kluth LA, Abdollah F, Xylinas E, et al. Clinical nodal staging scores for prostate cancer: a proposal for preoperative risk assessment. Br J Cancer. 2014; 111:213–219. [PubMed: 25003663]
4. Tilki D, Mandel P, Seeliger F, et al. Salvage lymph node dissection for nodal recurrence of prostate cancer after radical prostatectomy. J Urol. 2015; 193:484–490. [PubMed: 25180792]
5. Karnes RJ, Murphy CR, Bergstralh EJ, et al. Salvage lymph node dissection for prostate cancer nodal recurrence detected by 11C-choline positron emission tomography/computerized tomography. J Urol. 2015; 193:111–116. [PubMed: 25150640]
6. Singhal S The Future of Surgical Oncology: Image-Guided Cancer Surgery. JAMA Surg. 2016; 151:184–185. [PubMed: 26765107]
7. Manny TB, Patel M, Hemal AK. Fluorescence-enhanced robotic radical prostatectomy using real-time lymphangiography and tissue marking with percutaneous injection of unconjugated indocyanine green: the initial clinical experience in 50 patients. Eur Urol. 2014; 65:1162–1168. [PubMed: 24289911]
8. Nguyen DP, Huber PM, Metzger TA, et al. A Specific Mapping Study Using Fluorescence Sentinel Lymph Node Detection in Patients with Intermediate- and High-risk Prostate Cancer Undergoing Extended Pelvic Lymph Node Dissection. Eur Urol. 2016; 70:734–737. [PubMed: 26856960]
9. Ramirez-Backhaus M, Mira Moreno A, Gomez Ferrer A, et al. Indocyanine Green Guided Pelvic Lymph Node Dissection: An Efficient Technique to Classify the Lymph Node Status of Patients with Prostate Cancer Who Underwent Radical Prostatectomy. J Urol. 2016; 196:1429–1435. [PubMed: 27235788]

10. Yuen K, Miura T, Sakai I, Kiyosue A, Yamashita M. Intraoperative Fluorescence Imaging for Detection of Sentinel Lymph Nodes and Lymphatic Vessels during Open Prostatectomy using Indocyanine Green. J Urol. 2015; 194:371–377. [PubMed: 25584996]
11. Chennamsetty A, Zhumkhawala A, Tobis SB, et al. Lymph Node Fluorescence During Robot-Assisted Radical Prostatectomy With Indocyanine Green: Prospective Dosing Analysis. Clin Genitourin Cancer. 2016.
12. Hruby S, Englberger C, Lusuardi L, et al. Fluorescence Guided Targeted Pelvic Lymph Node Dissection for Intermediate and High Risk Prostate Cancer. J Urol. 2015; 194:357–363. [PubMed: 25896557]
13. Inoue S, Shiina H, Arichi N, et al. Identification of lymphatic pathway involved in the spreading of prostate cancer by fluorescence navigation approach with intraoperatively injected indocyanine green. Can Urol Assoc J. 2011; 5:254–259. [PubMed: 21801682]
14. van der Poel HG, Buckle T, Brouwer OR, Valdes Olmos RA, van Leeuwen FW. Intraoperative laparoscopic fluorescence guidance to the sentinel lymph node in prostate cancer patients: clinical proof of concept of an integrated functional imaging approach using a multimodal tracer. Eur Urol. 2011; 60:826–833. [PubMed: 21458154]
15. van Leeuwen FW, Hruby S. Fluorescence guidance during radical prostatectomy. Eur Urol. 2014; 65:1169–1170. [PubMed: 24411990]
16. Lee JY, Thawani JP, Pierce J, et al. Intraoperative Near-Infrared Optical Imaging Can Localize Gadolinium-Enhancing Gliomas During Surgery. Neurosurgery. 2016; 79:856–871. [PubMed: 27741220]
17. Jiang JX, Keating JJ, Jesus EM, et al. Optimization of the enhanced permeability and retention effect for near-infrared imaging of solid tumors with indocyanine green. Am J Nucl Med Mol Imaging. 2015; 5:390–400. [PubMed: 26269776]
18. Singhal S, Nie S, Wang MD. Nanotechnology applications in surgical oncology. Annu Rev Med. 2010; 61:359–373. [PubMed: 20059343]
19. Okusanya OT, Holt D, Heitjan D, et al. Intraoperative near-infrared imaging can identify pulmonary nodules.Ann Thorac Surg. 2014; 98:1223–1230. [PubMed: 25106680]
20. Keating JJ, Nims S, Venegas O, et al. Intraoperative imaging identifies thymoma margins following neoadjuvant chemotherapy. Oncotarget. 2016; 7:3059–3067. [PubMed: 26689990]
21. Keating J, Tchou J, Okusanya O, et al. Identification of breast cancer margins using intraoperative near-infrared imaging. J Surg Oncol. 2016; 113:508–514. [PubMed: 26843131]
22. Keating J, Newton A, Venegas O, et al. Near-Infrared Intraoperative Molecular Imaging Can Locate Metastases to the Lung. Ann Thorac Surg. 2017; 103:390–398. [PubMed: 27793401]
23. Holt D, Okusanya O, Judy R, et al. Intraoperative near-infrared imaging can distinguish cancer from normal tissue but not inflammation. PLoS One. 2014; 9:e103342.
24. Wit EM, Acar C, Grivas N, et al. Sentinel Node Procedure in Prostate Cancer: A Systematic Review to Assess Diagnostic Accuracy. Eur Urol. 2016.
25. Buckle T, Brouwer OR, Valdes Olmos RA, van der Poel HG, van Leeuwen FW. Relationship between intraprostatic tracer deposits and sentinel lymph node mapping in prostate cancer patients. J Nucl Med. 2012; 53:1026–1033. [PubMed: 22645296]
26. Roy J, Nguyen TX, Kanduluru AK, et al. DUPA conjugation of a cytotoxic indenoisoquinoline topoisomerase I inhibitor for selective prostate cancer cell targeting. J Med Chem. 2015; 58:3094–3103. [PubMed: 25822623]
27. Sonn GA, Behesnilian AS, Jiang ZK, et al. Fluorescent Image-Guided Surgery with an Anti-Prostate Stem Cell Antigen (PSCA) Diabody Enables Targeted Resection of Mouse Prostate Cancer Xenografts in Real Time. Clin Cancer Res. 2016; 22:1403–1412. [PubMed: 26490315]
28. Nakajima T, Mitsunaga M, Bander NH, et al. Targeted, activatable, in vivo fluorescence imaging of prostate-specific membrane antigen (PSMA) positive tumors using the quenched humanized J591 antibody-indocyanine green (ICG) conjugate. Bioconjug Chem. 2011; 22:1700–1705. [PubMed: 21740058]

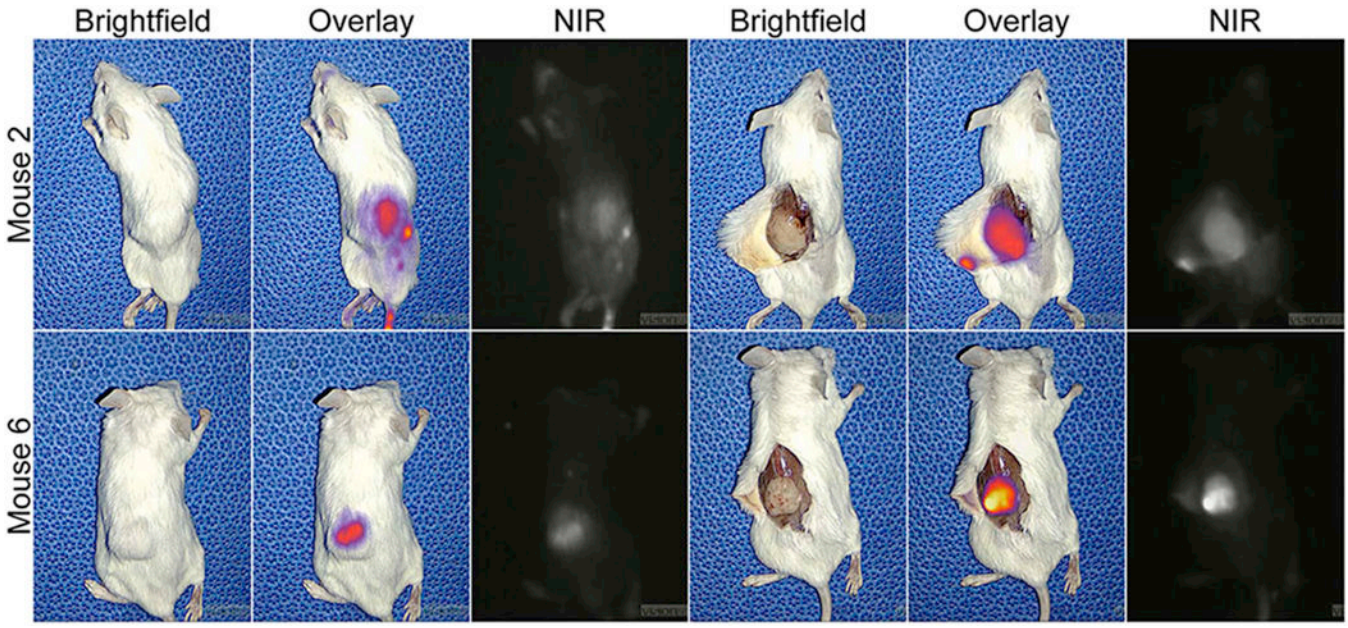

Figure 1.
NIR fluorescence of two mouse prostate cancer xenografts

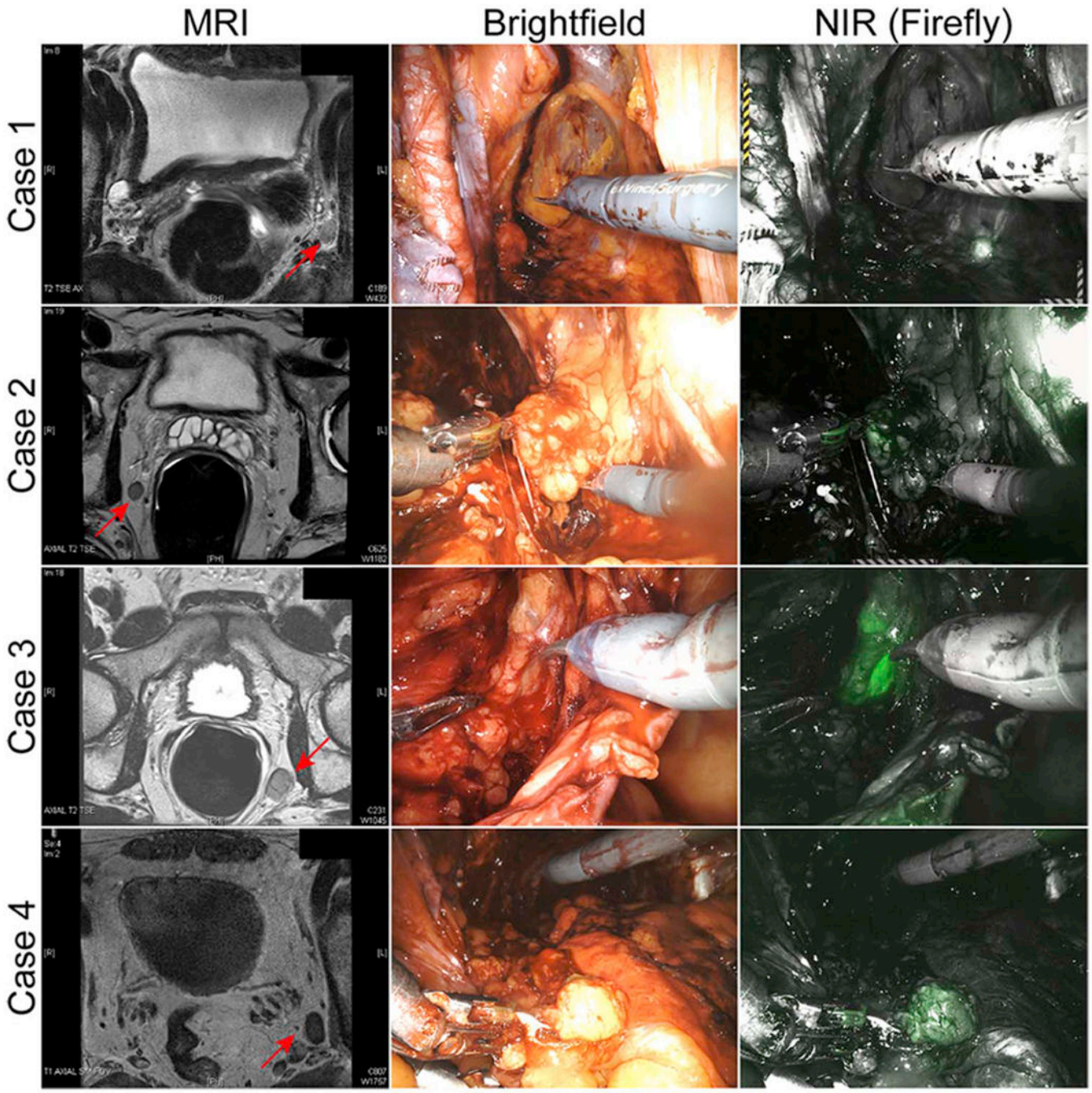

Figure 2.
Preoperative MRI scans and *In vivo* NIR fluorescence of the lymphadenopathies

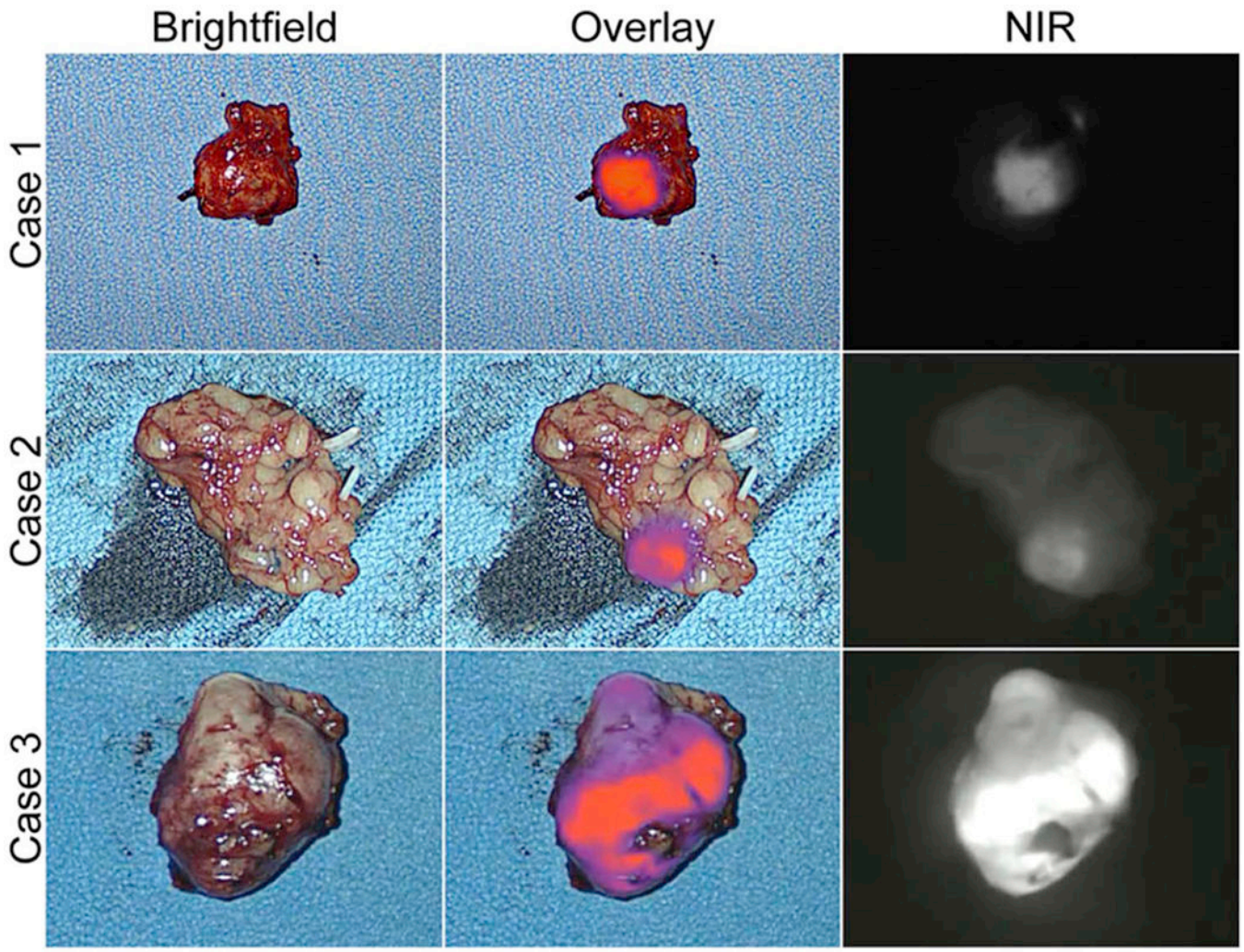

Figure 3.
Ex vivo NIR fluorescence of the lymphadenopathy specimens

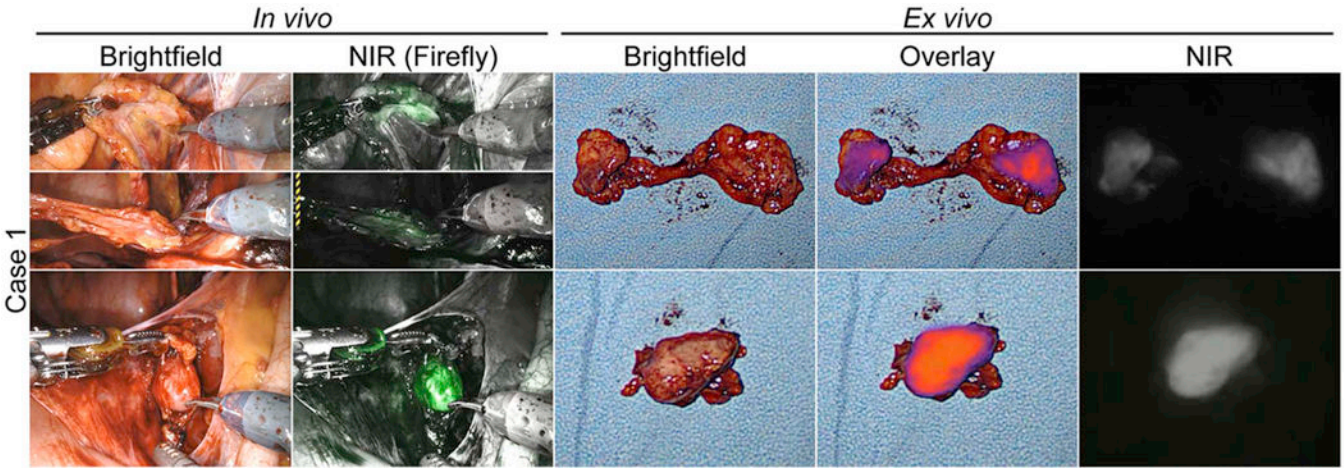

Figure 4.

In vivo and *ex vivo* NIR fluorescence of two additional LNM specimens in Case 1